Available online at www.sciencedirect.com
SCIENCE DIRECT
Sensors and Actuators A 120 (2005) 370–382
SENSORS AND ACTUATORS A PHYSICAL
www.elsevier.com/locate/sna

Design and fabrication of a hybrid silicon three-axial force sensor for biomechanical applications

Lucia Beccai [a,*], Stefano Roccella [b], Alberto Arena [a], Francesco Valvo [a], Pietro Valdastri [a], Arianna Menciassi [a], Maria Chiara Carrozza [b], Paolo Dario [a,b]

[a] *CRIM—Centre for Research In Microengineering, Polo Sant'Anna Valdera—Scuola Superiore Sant'Anna, Viale Rinaldo Piaggio 34, 56025 Pontedera, PI, Italy*
[b] *ARTS Lab—Advanced Robotics Technology and Systems Laboratory, Polo Sant'Anna Valdera—Scuola Superiore Sant'Anna, Viale Rinaldo Piaggio 34, 56025 Pontedera, PI, Italy*

Received 7 July 2004; received in revised form 16 December 2004; accepted 2 January 2005
Available online 5 February 2005

Abstract

This paper presents the design and development of a silicon-based three-axial force sensor to be used in a flexible smart interface for biomechanical measurements. Normal and shear forces are detected by combining responses from four piezoresistors obtained by ion implantation in a high aspect-ratio cross-shape flexible element equipped with a 525 μm high silicon mesa. The mesa is obtained by a subtractive dry etching process of the whole handle layer of an SOI wafer. Piezoresistor size ranges between 6 and 10 μm in width, and between 30 and 50 μm in length. The sensor configuration follows a hybrid integration approach for interconnection and for future electronic circuitry system integration. The sensor ability to measure both normal and shear forces with high linearity (≅99%) and low hysteresis is demonstrated by means of tests performed by applying forces from 0 to 2 N. In this paper the packaging design is also presented and materials for flexible sensor array preliminary assembly are described.

Keywords: Three-axial; Force; Microsensor; Hybrid; Biomechanics

1. Introduction

Silicon-based sensors perform quantitative measurements with high reliability and they can be an attractive solution for biomechanical measurements when coupled with suitable and reliable packaging solutions. Miniature three-axial force sensors can be successfully used for biomechanical measurements in the field of prosthetics. In fact, it is well known that one of the main causes of failure of a prosthesis for lower limb above-knee (AK) amputees, is the bad fitting of the socket to the stump. The prosthesis comfort is highly conditioned by normal and shear forces that arise at the interface between the socket surface and the stump [1,2]. Hence, it is of fundamental importance to measure the entity and distribution of such forces during user locomotion in order to evaluate the fitting degree of the socket and to optimize its shape, thus reducing the entity of the skin damage. In order to address the problem of performing such biomechanical measurements in real time, when the user is wearing the prosthetic device, it is necessary to develop miniature sensors appropriate to be incorporated in the socket without impairing normal and comfortable motion control.

In this paper we present the design and fabrication of the silicon microsensor that we have developed for the specific prosthetic purpose but that can be applied in other medical applications where the keyword requirements are three-axial force measurement and miniaturization. The device has been designed in order to develop a flexible smart interface to be used to detect the forces to which the stump skin tissue is sub-

* Corresponding author. Tel.: +39 050 883 419; fax: +39 050 883 497.
E-mail address: l.beccai@crim.sssup.it (L. Beccai).

0924-4247/$ – see front matter © 2005 Elsevier B.V. All rights reserved.
doi:10.1016/j.sna.2005.01.007

jected while in contact with the socket worn by AK amputees. In addition, the mechanical characteristics of the sensor have also been assessed as appropriate for the sensory system of artificial hands [3–7].

Concerning the state of the art of three-axial or shear force silicon-based sensors, they have been developed mainly using the piezoresistive and capacitive principles. Yao et al. [8] developed a three-axial force sensor integrating eight piezoresistors in a silicon bossed-diaphragm structure. Chu et al. [9] reported a three-axial tactile sensor based on the differential capacitive principle. Wang and Beebe [10] developed a normal and shear force sensitive device by integrating four piezoresistors in a silicon square diaphragm equipped with an EPON SU-8 mesa and using them as independent strain gauges. Bütefisch et al. [11] built a square boss silicon membrane with 24 embedded piezoresistors and a stylus for mechanical characterisation of micromaterials. Kane et al. [12] reported a shear-stress sensor array (64×64 elements) capable of high-resolution imaging. The sensors are developed with a fully CMOS compatible fabrication process and consist of a shuttle plate suspended over an etched pit by four beams in which polysilicon piezoresistors are integrated. Bartsch et al. [13] adapted the tactile microsensor reported by Kane et al. to a millimetre-scale silicon micromachined force sensor to measure the ground reaction microforces produced by a cockroach in order to obtain useful parameters for biomimetic robot design. Jin and Mote [14] integrated 12 piezoresistors in a polysilicon cross-beam to implement a three-component microforce sensor. Jiang et al. [15] fabricated a shear stress sensor skin to perform 2D profiling in aerodynamics, and Xu et al. [16] recently reported improvements of this technology for the application in unmanned aerial vehicles. Moreover, a shear-stress type sensor has been reported [17] for the AK prosthesis application. It consists of a $3\,\text{mm} \times 3\,\text{mm} \times 300\,\mu\text{m}$ square diaphragm, built by bulk micromachining, with two implanted piezoresistors and a $1.2\,\text{mm} \times 1.2\,\text{mm} \times 3\,\mu\text{m}$ silicon dioxide protuberance.

Ideally, in order to be used for human interface measurement, sensors should satisfy requirements as: linearity, low hysteresis, low creep; low temperature sensitivity; flexibility; small thickness; large range of measurement; repeatability (durability); be unobtrusive, easy to use and cost effective [18]. Even if they hold considerable promise, the existing types of three-axial force silicon sensors are not likely to satisfy all requirements. Furthermore, from the technological point of view, they are generally equipped with a dome or a mesa built with various techniques and materials. In general wet bulk micromachining is the preferred technology to create silicon bosses on flexible structures [8,11], but also additive processes (like SU-8 deposition) have been employed to create vertical structures [10]. Previously microfabricated components (silicon and not-silicon) have also been bonded [9] or attached [11] to sensors.

In the three-axial force sensor presented in this paper, the fabrication technology and materials used allow the implementation of a silicon high aspect-ratio structure with an integrated silicon mesa used for the transmission of the force to a flexible tethered structure. It is obtained by a subtractive etching process of the whole wafer; thus, additional bonding or attaching steps, using additional materials between the mesa and the flexible structure, are not necessary.

Four piezoresistors are used independently in order to measure the three components of applied forces through a resistance change, and the sensor cross-shape guarantees the mechanical decoupling of the shear components of the applied load. Verification of sensor response is presented in this paper as a preliminary result of device characterization. The sensor design follows a hybrid approach [19,20], allowing the possibility of future smart sensor implementation at low-cost since sensor design and fabrication process can remain unaltered.

Research attention has been paid in overcoming problems as silicon fragility and providing durable sensor systems [15,18,21]. In this work the design of the proposed three-axial force sensor has been performed simultaneously to the design of its packaging with the aim of developing a flexible smart interface for biomechanical measurements. The implemented hybrid silicon microsystem allows the assembling of an array of devices in a flexible substrate. The flexible array is embedded in skin like materials that act as a mechanical interface between the sensor array and the external world.

2. Sensor design

The sensor consists of two parts as illustrated in Fig. 1, the sensing chip and the carrier chip, connected by flip-chip bonding.

The design choice of using a support chip bonded to the sensing element is related to the fact that the physical interaction with the outer world occurs at one side, while the electrical connections must be performed at the opposite side of the sensible structure. The combination of a carrier chip and the flip-chip technology allows to have horizontal electri-

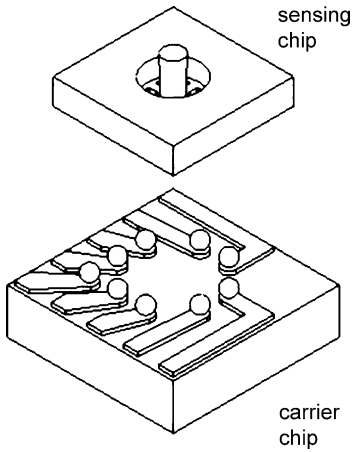

Fig. 1. Sensor structure.

cal connections and low total thickness, which is a major requirement for flexible skin implementation. The carrier chip provides a rigid support for the sensor and flat back surface for easy positioning.

The hybrid sensor configuration is highly flexible since it is possible to integrate signal processing electronics that can be changed at any time just by replacing the support chip, thus allowing easy customization for different applications. In this way, it is possible to obtain a smart sensor just by means of an assembling step, with no need to change its design nor its fabrication process.

2.1. Mechanical structure

The sensor consists of a flexible sensing structure with four tethers whose axes are perpendicular to each other in a cross-shape, and a cylindrical mesa, located at the cross center, that transmits the force.

An external force applied to the sensor can be resolved into its three components F_n, F_x, F_y as shown in Fig. 2. Ideally, thanks to the sensor cross-shape, F_n induces symmetrically distributed stresses in the four tethers while F_x and F_y induce stresses in the tethers exclusively along their direction of application. Thus, the shear components of the applied load are mechanically decoupled. In order to be able to transfer the shear loads to the tethers, the mesa emerges from the rest of the structure.

2.1.1. Dimensioning

The dimensions of the sensor have been defined on the basis of the estimation of the contact forces arising at the stump/socket interface during the amputee's locomotion phase. The maximum pressure applied locally at the socket has been estimated as $P = 0.329$ MPa that corresponds to a normal load $F_{normal} = 0.26$ N when considering a contact circular area of 1 mm diameter. With an average friction coefficient between stump and socket $\mu \cong 0.8$, the maximum shear stress that is applied locally is $\tau = \mu P = 0.26$ MPa corresponding to a shear load $F_{shear} = 0.21$ N.

The sensor is based on the piezoresistive effect and the fractional change in resistance is given by [22]

$$\frac{\Delta R}{R} = \pi_l \sigma_l + \pi_t \sigma_t \quad (1)$$

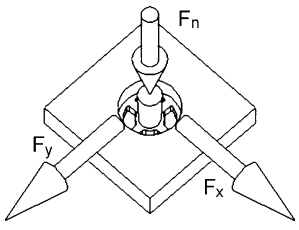

Fig. 2. Mechanical structure of the sensor where the applied forces are indicated with F_n for the normal force, while F_x and F_y are the two components of the shear load.

where σ_l and σ_t are the longitudinal and the transversal stress components induced in the resistor R, and π_l and π_t are the longitudinal and transversal piezoresistance coefficients. The methodology consisted in designing a preliminary mechanical structure, simulating the mechanical stresses in the silicon device by means of finite element analysis (FEA) simulation tools (ANSYS® 5.7) in order to obtain a numerical value of $\Delta R/R \cong 3\%$ that fulfills low power dissipation requirements of the device.

The mechanical structure of the sensor has been defined following an iterative process. A file batch has been generated in which the main dimensional parameters, the elastic orthotropic characteristics of the silicon material and the Eq. (1) have been inserted. The FEA outcome when a working load is applied is shown in Fig. 3.

The main mechanical features of the sensor have the dimensions shown in Fig. 4. The mesa is 525 μm high and emerges of 200 μm from the rest of the structure. A fillet radius and a step both at the tethers roots and at the base of the cylindrical mesa have been introduced, in order both to reduce the concentration of the stresses at sharp corners and to have a tethers cross-section gradual change, thus preventing fractures of the structure.

The tethers thickness has been chosen so that the sensor ultimate load (7 N) is close to the maximum load that has been considered for the design of tactile sensors to be applied in artificial hands [3–7]; this turns out from the load at the hands fingertips during precision grip in humans [23].

The mechanical strength of the sensor has been evaluated by progressively varying the three components of the resulting force applied on top of the mesa up to the maximum acceptable values of the adopted strength criteria. FEM analysis with a force of 7 N applied at different angles respect to the sensor axis has been performed. With such force value the sensor is loaded to the maximum strength that is evaluated by considering the silicon yield strength (2.8–7 GPa) [24] thus the calculated safety factor of the design is approximately 15.

2.2. Piezoresistors

In order to obtain maximum sensitivity, regions of high stress have been identified and piezoresistors dimensions and position have been determined accordingly.

Four bar shape p-type piezoresistors are integrated in the tethers oriented in the ⟨1 1 0⟩ direction since the piezoresistive coefficient has a maximum in that direction, thus the longitudinal and transversal stresses, σ_l and σ_t of each piezoresistor are the stresses along the parallel and perpendicular direction to the tether axis, respectively.

It results from FEA that the stresses have a maximum at the tethers roots. A higher maximum is at the base of the mesa, as shown in Fig. 3, but it is not reliable for design since such high stress area is next to the mesa sharp edge, that is a singularity region to be modeled since a fillet radius cannot be introduced for technological constraints. The piezoresistors placement is optimal for any applied load arbitrarily oriented respect to the

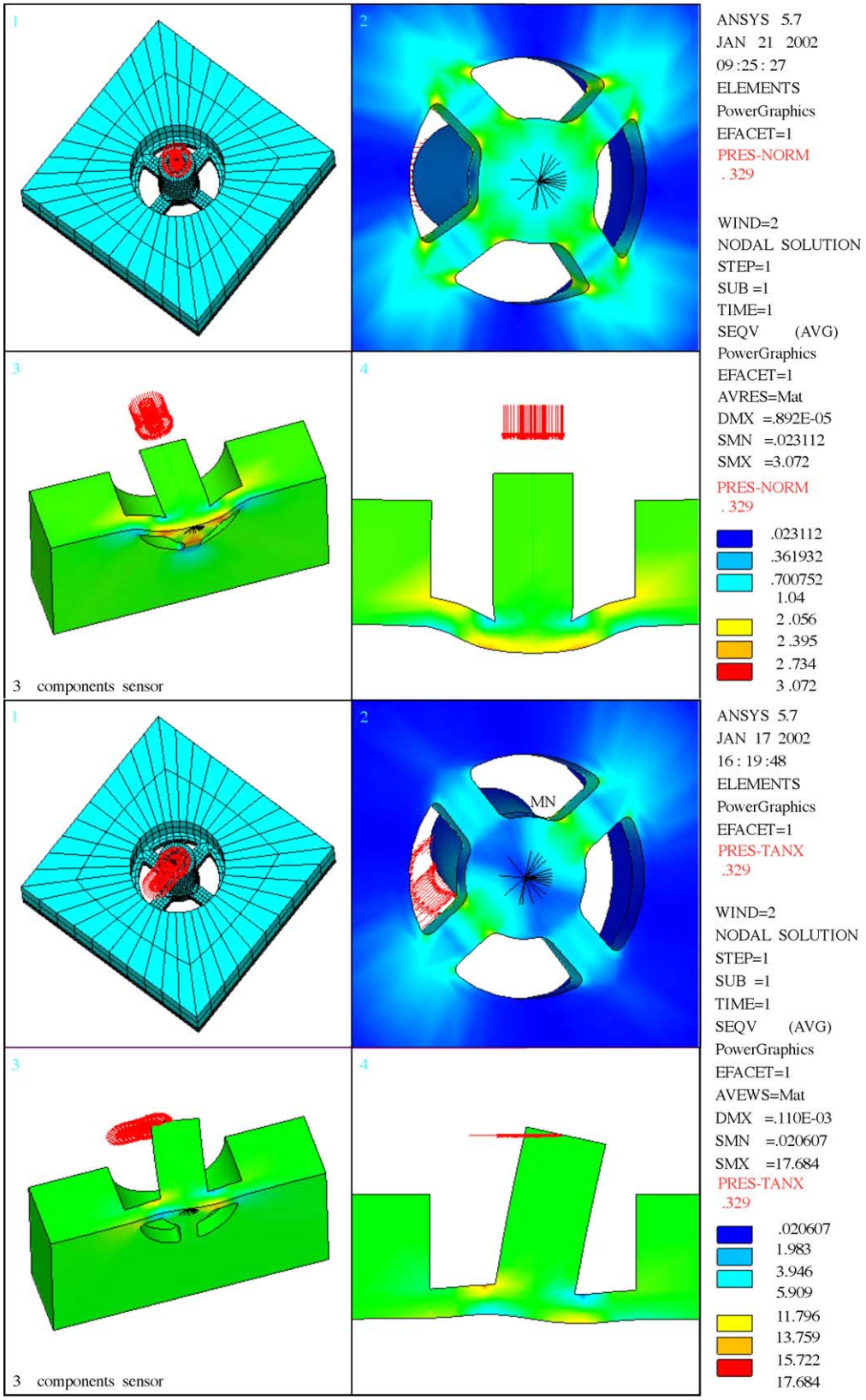

Fig. 3. FEA performed by means of ANSYS® 5.7 with an applied load of 0.329 MPa.

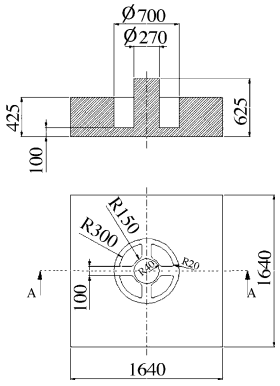

Fig. 4. Detail drawing of the sensor with dimensions.

sensor, since the areas of maximum stress remain the same due to the sensor cross shape.

Considering a resistor R having area A_R, the piezoresistive sensitivity is given by $\Delta R/R$ per unit of applied force [25]

$$S_F = \left.\frac{\Delta R}{R}\right|_{\text{unit force}} = \frac{1}{A_R}\int_0^{A_R} (\pi_l\sigma_l + \pi_t\sigma_t)\,\delta A \tag{2}$$

where ΔR corresponds to the resistance change for an applied force.

The piezoresistors dimensions have been chosen much smaller than the tethers dimensions so that stresses can be considered constant in the piezoresistors. A low doping concentration is used in order to achieve a high piezoresistive coefficient. Being for p-type piezoresistors $\pi_l = \pi_t \cong \pi_{44}/2$ where $\pi_{44} = 138 \times 10^{-11}$ Pa for low doping levels [26,27]; S_F becomes

$$S_F = \frac{\pi_{44}}{2}(\sigma_l - \sigma_t)|_{\text{unit force}} \tag{3}$$

A higher sensitivity is achieved when σ_t is minimized. It has been verified with FEA that σ_t is one order of magnitude smaller than σ_l and the piezoresistors have been designed with a width smaller than their length so that it can be assumed that $\sigma_t \ll \sigma_l$ thus

$$S_F = \frac{\pi_{44}\sigma_l}{2F} \tag{4}$$

where F is the applied force.

Different configurations of piezoresistors have been designed. Width and length range from 6 to 10 μm and from 30 to 50 μm, respectively. The sensitivity to the applied load and the mechanical decoupling effect of the sensor depends on the longitudinal and transversal position of each piezoresistor. The technological process parameters have been set in order to obtain a thin piezoresistor. As a thinner piezoresistor has a higher electrical resistance, it is desirable to obtain small thickness and short length in order to increase sensitivity and to obtain low power consumption.

3. Sensor fabrication

The fabrication process has been carried out at the Institute of Microtechnology in Mainz, Germany. The sensing element has been built with an SOI wafer and applying the Advanced Silicon Etching (ASE™) technology. This deep dry process etches anisotropically the silicon substrate on both sides conferring the device its particular 3D mechanical configuration equipped with a silicon cylinder mesa at its center.

The SOI wafer is n-type and with a (1 0 0) surface orientation. It has a device layer and a handle layer with a thickness of 100 and 525 μm, respectively, and separated by a 500 nm thick buried oxide layer. The ASE™ tool used is the multiplex inductively coupled plasma etching system from Surface Technology Systems (Newport, UK). The method uses the time/gas switched Bosch process [28] with a high density fluorine plasma chemistry. The silicon is etched preferentially in vertical direction thus resulting in an anisotropic etch profile. The etch rates and switching times strongly depend on the depth of silicon that is removed; in order to optimize the side wall profile and the edge quality of the silicon structures, switching times and gas flows have been varied.

The nine-mask fabrication process is divided in two main sequences for the processing of the wafer device layer and handle layer, respectively. The main fabrication steps are shown in Fig. 5.

At first the device layer is processed after thermal oxidation of the wafer and resist is used to protect the layer of thermal oxide on the handle layer. The p-type piezoresistors are obtained by ion implantation of Boron with a dose of 1.5×10^{15} cm^{-3}, energy of 40 kV and a subsequent ion activation process at 900 °C of 30 min in an atmosphere of

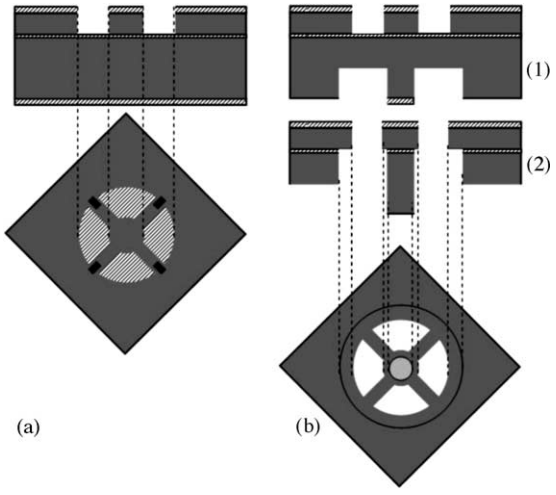

Fig. 5. Schematization of the sensor main fabrication steps. (a) Device layer process: after implantation of the piezoresistors, fabrication of Al interconnections and Au pads electrochemical growth, 100 μm thick tethers are fabricated by advanced silicon etch (ASE™). (b) Handle layer process: a silicon step of 325 μm (1) and one of 200 μm (2) are fabricated with the double-level ASE™ process that yields the 525 μm high cylindrical mesa emerging 200 μm from the rest of the structure.

oxygen and nitrogen. The diffusion time is set short in order to achieve a shallow doping profile. After contacts and Al lines are implemented, the Au pads are grown with an electrochemical process. The latter starts from an aluminum layer of 1 μm that undergoes a zincating process, electroless deposition of nickel and final immersion into gold for electrochemical growth. The distance between the pads and their dimensions must have been defined based on the flip-chip packaging requirements.

The tethers of the sensor flexible structure are then realized as a result of an ASE™ step that removes the 100 μm thickness of the SOI device layer (called "shallow process" [29]).

Resist and the buried oxide layer are used as mask and etch stop materials, respectively. After the device layer has been processed the surface of the wafer presents a topography with a silicon step of 100 μm corresponding to the thickness of the tethers (see Fig. 6).

The processing of the handle layer of the wafer is performed (three mask process) by applying a double level ASE™ to obtain the double level pattern of the sensor. A first ASE™ removes 325 μm of silicon and AZ resist is used as a mask, while timing is used to stop the etch. Then the resist is removed with a dry etch, and a second ASE™ removes 200 μm of silicon using a thermal oxide mask of about 1.5 μm and the buried oxide layer as etch stop. Both ASE™ etches are "deep processes" [29].

Before performing the second etch step a protection resist layer has been deposited on the wafer device layer in order to prevent the contamination of the plasma gas during the ASE™ handle layer etching with the He cooling gas from the device layer of the wafer. In addition since the last etch causes the breakage of the buried oxide layer the resulting suspended structure is subjected to high stress and a protection layer is needed for its mechanical stabilization. Fig. 7 illustrates a SEM image of the fabricated sensor while in Fig. 8 the double level structure of the sensor is shown through a cross-section of the same.

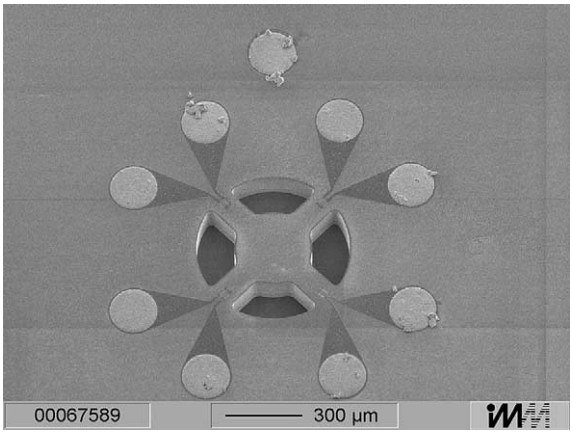

Fig. 6. SEM picture of structures at the wafer front-side presenting a silicon step of 100 μm.

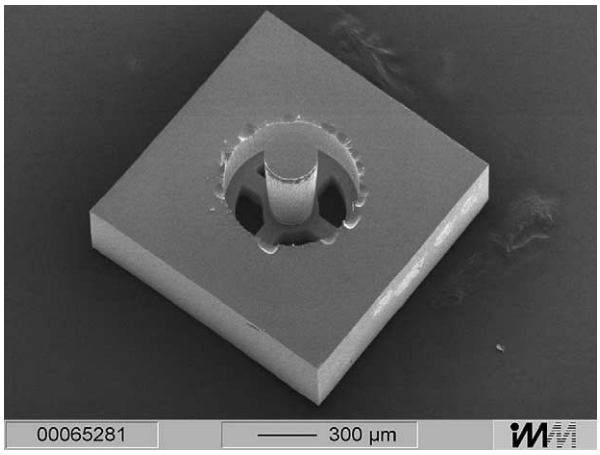

Fig. 7. SEM picture of the sensor structure.

The wafers for the carrier chips were again processed at the Institute of Microtechnology in Mainz, Germany. A lift-off process has been used to obtain Au pads with a layout corresponding to the pads layout on the sensing chip. Al lines connect these pads to the Au pads positioned at the edges of the chip, to ensure the electrical connection with the outer world.

3.1. System assembly

Once the fabrication process is completed and the chips have been diced, the released carrier chip and the sensing element are assembled. The final sensor dimensions are 2.3 mm × 2.3 mm × 1.3 mm.

The sensing and the carrier chips have been designed in order to be bonded via flip-chip. A conductive polymeric glue (H37MP, Epotek Technology, Billerica, MA, USA) is used to perform the bond between the corresponding pads of the two chips; a robotic station devoted to dispense the glue and to manipulate and to precisely position the chips has been set-up.

The spacing between the sensing element and the silicon substrate is constrained by the polymer bond, and it must be

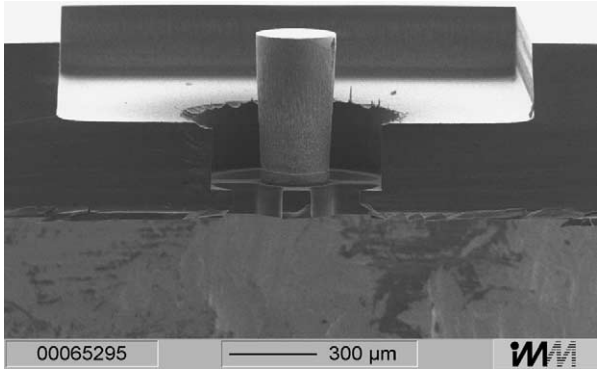

Fig. 8. Cross-section at one tether after the last ASE™ step.

constant for the sensor to properly detect the three components of applied forces.

Although the glue is dispensed in fixed amounts with an automatic, reliable system, curing of the glue may cause the sensing chip to be not perfectly parallel to the support chip. After curing, however, the gap has been measured and it has been verified that no significant error has been introduced in the parallelism of the chips. The spacing guarantees the mobility of the suspended tethers.

4. Preliminary characterization methods

In order to demonstrate and investigate the ability of the sensor to measure both normal and shear forces, preliminary characterization experiments have been performed using a purposely developed characterization workstation. The tests have been performed on sensors with 6 μm × 30 μm implanted piezoresistors and they consist of normal and tangential compression tests on the top of the cylindrical mesa and in the registration of the variation in resistance of each of the four piezoresistors.

4.1. Read out electronics

The conditioning electronics have been designed in order to have an output voltage proportional to the fractional change in resistance $\Delta R/R$. Each resistor ($R \cong 1\,\text{k}\Omega$) is independently conditioned, using a Wheatstone bridge configuration with two precision 1 kΩ resistors and one trimmer, in order to adjust the initial offset level. The bridge output signal is then led to an instrumentation amplifier (AD620, Analog Devices, Norwood, MA, USA). The amplifier gain A can be adjusted from 1 to 1000. The input voltage of the circuit is $V_{IN} = 3.3$ V. The block diagram of the signal conditioning circuit for one piezoresistor is shown in Fig. 9.

Considering a balanced bridge where $R_1 = R_2 = R_3 = R$ the output of the circuit is

$$V_{OUT} = A(V^+ - V^-) = AV_{IN}\frac{\Delta R}{4R + 2\Delta R} \approx AV_{IN}\frac{\Delta R}{4R} \quad (5)$$

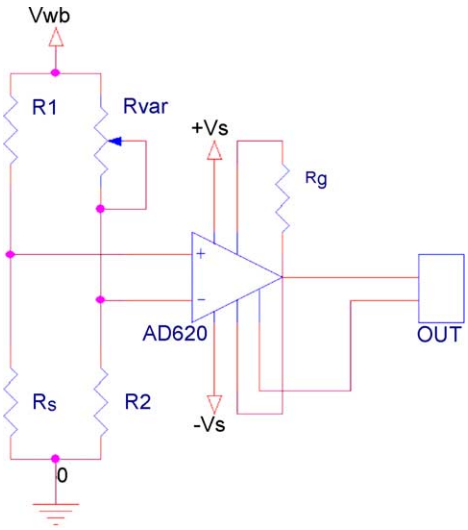

Fig. 9. Diagram of the signal conditioning circuit.

Thus, the resistance variation can be obtained from the output voltage. The power consumption obtained using the signal conditioning circuit shown above, is about 10–11 mW per one sensor. A more sophisticated circuitry can be designed in order to further decrease the power consumption of the sensor.

4.2. Experimental set-up

The characterization apparatus is shown in Fig. 10 and consists of a loading structure, a double vision system for probe-sensor alignment, signal conditioning electronic circuitry, data acquisition, and a PC workstation for data analysis.

The load is applied to the sensor by a needle shaped end-effector, screwed to the final part of a subminiature load cell, Model 11 (full scale of 1000 g) from Sensotec (Columbus, OH, USA). This loading structure is mounted on a servo-controlled nanometric translation stage, with a DC servomotor (111-1DG from PI, Karlsruhe, Germany), that imposes a force on the sensor mesa, with a user defined speed. The dc motor is equipped with a high resolution encoder featuring a

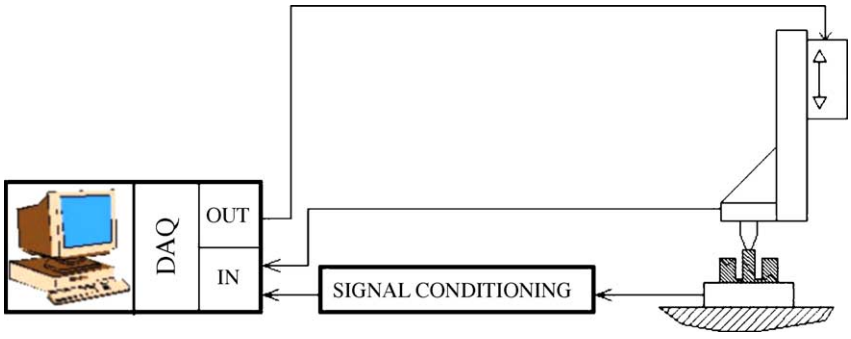

Fig. 10. A schematization of the characterization apparatus.

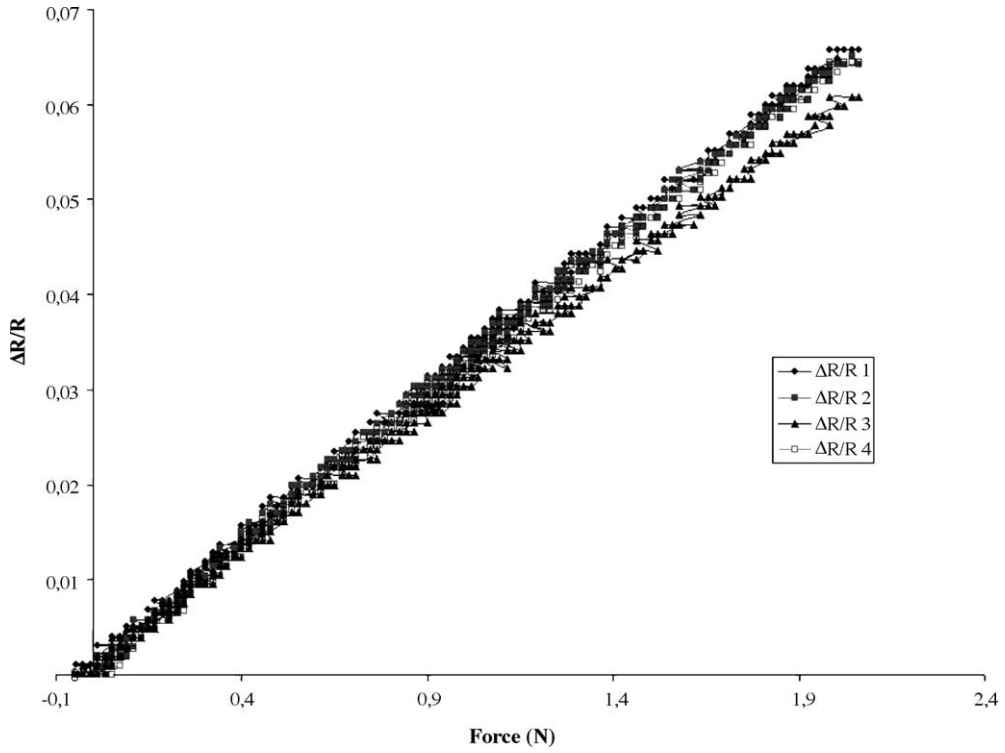

Fig. 11. Loading response of the sensor.

resolution of 7 nm per count and is connected to a controller (PI Mercury C-860.10) that is interfaced to the PC workstation.

The nanometric slider is fixed on *x–y–z* manual micrometric translation stage (PI M105), for rough positioning. This loading system is suitable for both normal and tangential load, just changing the orientation of the nanometric stage on the rough positioning system.

The sensor device is wire-bonded to a purposely developed steel support, which has air suction capabilities, in order to maintain the sensor in a fixed position during loading tests.

The four amplified signals from the sensor piezoresistors and the load cell output are acquired with a data acquisition (DAQ) card (AT-MIO-16E-10 from National Instruments, Austin, TX, USA), using a sample rate of 50 Hz. The instrumentation amplifier gain of each channel is selected in order to fit the input dynamic of the DAQ card.

The operator, through a graphical user interface purposely developed using LabView 7 Express (National Instruments), can impose a translation to the nanometric slider, and thus applies a load to the sensor while sampling the four sensor channels and the load cell output.

The alignment between the loading structure and the sensor mesa is performed using two fibre optic microscopes, VH5901 with 50× magnification from Keyence (Woodcliff Lake, NJ, USA) for alignment in *x*-direction, and KH2700 with 50× magnification from Hirox (Tokyo, Japan) for alignment in *y*-direction.

5. Experimental results and discussion

5.1. Normal load tests

These tests have been performed imposing a typical hysteresis cycle, obtained when an applied force is increasing from 0 to 2 N and decreasing back to zero at a translational constant speed of 1 μm/s along the *z*-direction. Each measurement was repeated five times to prove the reliability of the system.

Typical sensor outputs, in terms of fractional change in resistance $\Delta R/R$ versus loading force, in response to loading and unloading are plotted in Figs. 11 and 12, respectively. Fig. 13 represents the typical hysteresis cycle for one piezoresistor and it shows that hysteresis is negligible. The slope of the curves were extracted using a linear regression technique and represents the sensitivity $S_F = \frac{\Delta R/R}{F}$, as previously defined in Eq. (2). The resulting average sensitivity of the four piezoresistors that belong to the same sensor is $0.032 \pm 0.001\ N^{-1}$. The coefficient of determination, that quantifies the linearity of the curve as it is close to one, is found of 0.997 for all the piezoresistors outputs.

5.2. Shear load tests

Preliminary tangential tests have been carried out changing the orientation of the nanotranslator and using a purposely designed end effector screwed on the load cell terminal. Acquired data for the tangential compression tests are plotted in Fig. 14.

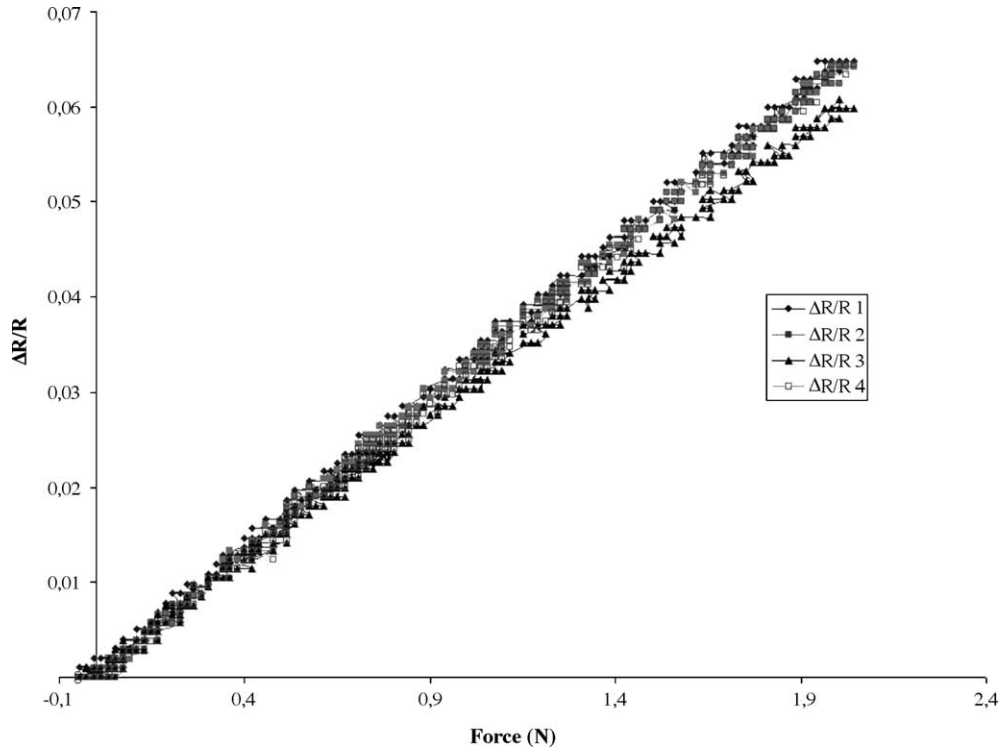

Fig. 12. Unloading response of the sensor.

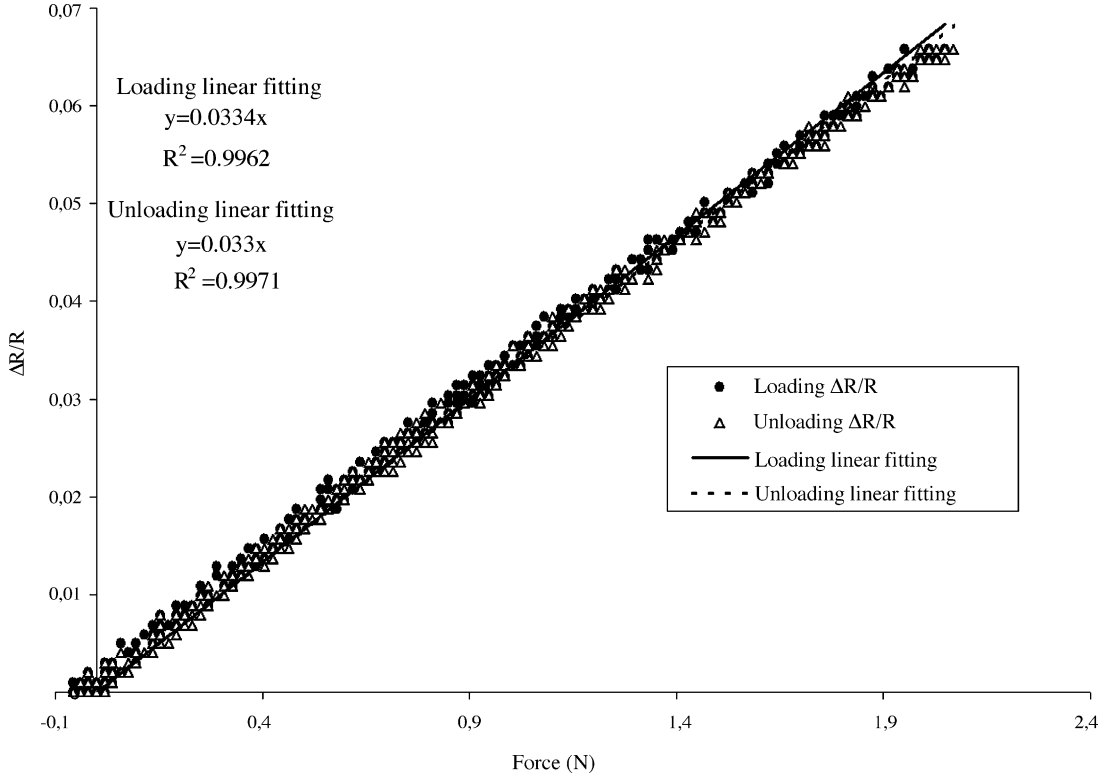

Fig. 13. Typical hysteresis cycle for one piezoresistor. The linear fitting and the relative equations are shown for the loading and unloading phases of the hysteresis cycle. The two linear graphs show very close slopes.

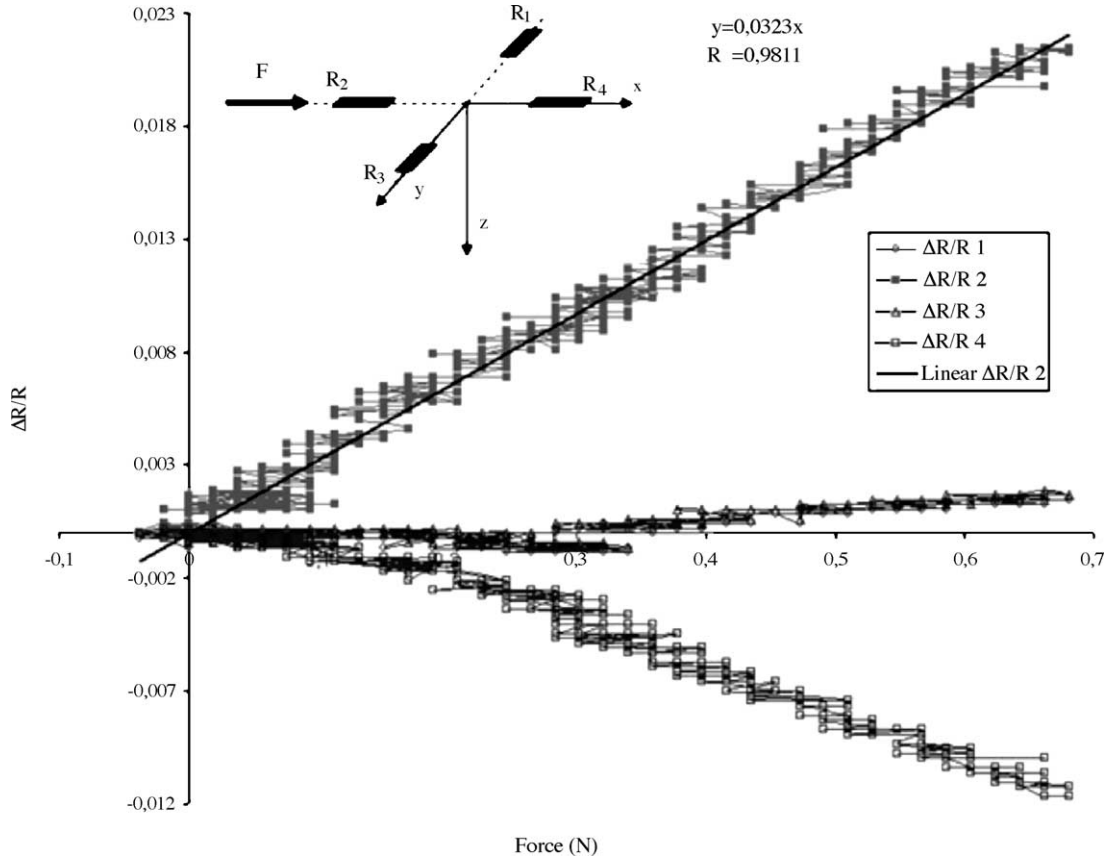

Fig. 14. Tangential loading response of the sensor.

The force was applied along the R_2–R_4 direction, so that, during the loading phase, R_4 and R_2 are stressed and compressed, respectively. The different behaviour of these two piezoresistors can be observed from experimental results, that also confirm that R_1 and R_3 are not significantly influenced. The shear sensitivity of R_2 was $0.0323\,\mathrm{N}^{-1}$ and the coefficient of determination was 0.9811, showing a high linearity of the sensor response.

6. Sensor packaging: design and preliminary results

A flexible packaging has been designed in order to obtain a smart interface for biomechanical measurements. Each sensor is considered as an element of an array positioned on a flexible substrate with printed circuits. The packaging must be robust and ensure protection to the silicon structure. At the same time, the packaging should not impair sensor operation

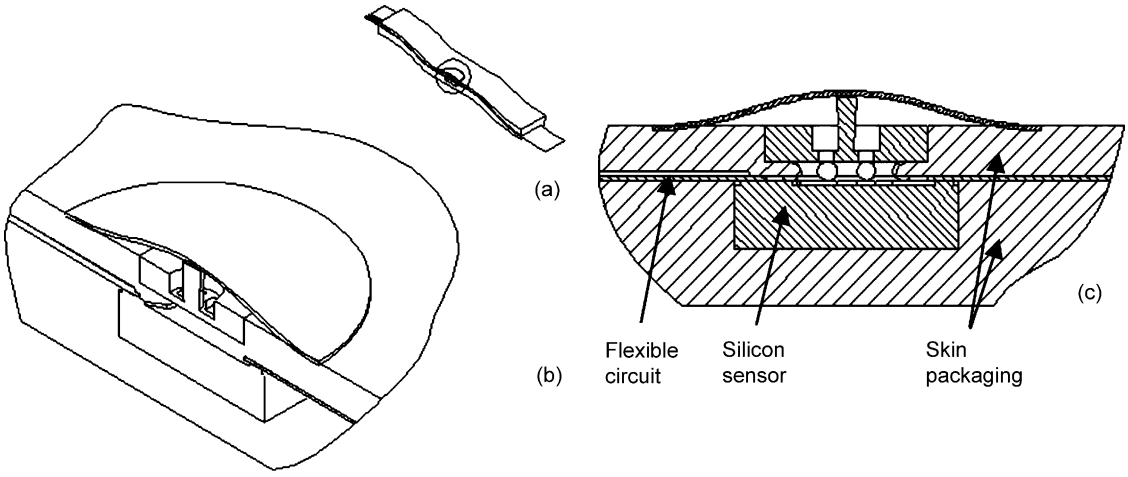

Fig. 15. Packaging design. A smart flexible interface (a) is obtained by assembling the sensor in different layers of polymeric materials and flexible connections (b). A section of the packaged sensor is shown in (c).

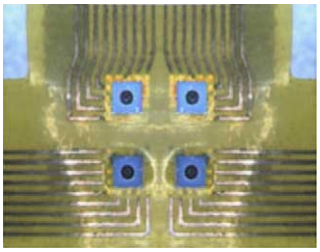

Fig. 16. A flexible circuit housing a 2×2 array of sensors.

while minimizing hysteresis and non-linearity effects. The design of the packaging is shown in Fig. 15.

Materials have been chosen and preliminary testing has been performed. Flexible Kapton (DuPont, Wilmington, DE, USA) circuits have been fabricated. Squared windows in the Kapton film are opened by laser cutting, large enough for the sensing element but not for the carrier chip. The sensor is then inserted into the film, positioned so that the copper lines of the circuit can contact the pads of the carrier chip while the sensing element protrudes from the Kapton film itself. A conductive glue produces the electrical connection.

A flexible circuit housing a 2×2 array of sensors has been fabricated (Fig. 16), in order to obtain a thin, flexible structure, capable of measuring interfacial loads. The array dimensions are 1 cm × 1 cm × 3 mm, thus obtaining a spatial resolution of 3.5 mm.

Preliminary investigations have been carried out in order to develop a skin-like layer that protects the upper part of the sensor and that also encapsulates the whole system. The materials to be used as encapsulant must be not toxic, but high biocompatibility is not required as the system will not be implanted. The cover layer must be soft and flexible. It must be thin enough in order to reduce mechanical filtering of the applied load and at the same time it must be able to withstand the cyclic mechanical action of the silicon cylinder sharp upper edge profile.

Polyurethane has been used as encapsulant, as it exhibits a set of favorable characteristics, such as excellent tensile strength properties, and it offers excellent chemical and abrasion resistance. Two kinds of polyurethane material have been used to perform preliminary packaging tests in order to verify material compatibility. MP1870Nat Polyurethane film from Stevens Urethane (Easthampton, MA, USA), having a thickness of 50.8 μm, has been used as a cover layer, while soft IE35A polyurethane from Innovative Polymers (St. Johns, MI, USA) as material to embed the sensor array strip. Preliminary tests show good adhesion between materials and high flexibility of the array strip.

7. Conclusions

A silicon three-axial force microsensor has been designed and fabricated. The device and its packaging have been designed in order to develop a flexible smart interface for biomechanical measurements. The advanced silicon etch process has allowed the implementation of a high aspect-ratio structure with an integrated silicon mesa used for the transmission of the force to a flexible tethered structure. The sensor has a hybrid configuration since it is equipped with a carrier chip in which conditioning and elaboration electronics can be integrated without changing the sensor fabrication process.

In order to verify sensor function, preliminary characterization tests have been performed by means of an experimental test bench encompassing a mono-axial load cell as core component. The piezoresistive based sensor has been tested by applying normal and tangential forces through the one-axis load cell. For an applied normal force between 0 and 2 N, the average sensitivity S_F of each piezoresistor is $0.032 \pm 0.001\,N^{-1}$ with a linearity of 99.7%. Preliminary tangential tests show a shear sensitivity of $0.0323\,N^{-1}$ with a linearity of 98.1%.

Future characterization tests will be performed with a three-axial load cell, in order to acquire the three components of the loading force and relate them to the sensor output by a calibration matrix, thus obtaining a complete characterization of the sensor.

Moreover, future work will consist in the optimization of the packaging method in order to develop a durable flexible smart interface according to the preliminary design shown in Fig. 15. The packaged sensor prototypes will be subjected to normal and shear load tests in order to compare the experimental results to the characterization results of the bare silicon sensors and verify that the packaging design and materials do not introduce significant hysteresis and non-linearity effects.

Acknowledgements

The research has been supported by the European Commission's "Improving Human Potential" (IHP) Programme in collaboration with the Institut fuer Mikrotechnik Mainz GmbH (IMM), Germany. The authors would like to thank R. Huber, W. Staab, L. Schmitt and F. Schmitz for their collaboration in the fabrication process of the sensor.

References

[1] M.W. Legro, G. Reiber, M. del Aguila, M.J. Ajax, D.A. Boone, J.A. Larsen, D.G. Smith, B. Sangeorzan, Issues of importance reported by persons with lower limb amputations and prostheses, J. Rehabil. Res. Develop. 36 (3) (1999).

[2] T.A. Krouskop, J. Brown, B. Goode, D. Winningham, Interface pressures in above knee sockets, Arch. Phys. Med. Rehabil. 68 (1987) 713–714.

[3] B. Massa, S. Roccella, R. Lazzarini, M. Zecca, M.C. Carrozza, P. Dario, Design and development of an underactuated prosthetic hand, in: Proceedings of the 2002 IEEE International Conference on Robotics and Automation, Washington, May, 2002.

[4] P. Dario, C. Laschi, A. Menciassi, E. Guglielmelli, M.C. Carrozza, L. Zollo, G. Teti, L. Beccai, F. Vecchi, S. Roccella, A Human-like robotic manipulation system implementing human models of

sensory-motor coordination, in: Proceedings of the IARP 2002, 3rd International Workshop on Humanoid and Human Friendly Robotics, Tsukuba, Japan, December 11–12, 2002, pp. 97–103.
[5] M.C. Carrozza, P. Dario, F. Vecchi, S. Roccella, M. Zecca, F. Sebastiani, The CyberHand: on the design of a cybernetic prosthetic hand intended to be interfaced to the peripheral nervous system, in: Proceedings of the ICRA 2003, International Conference on Intelligent Robot and Systems, Las Vegas, Nevada, October, 2003, pp. 2644–2647.
[6] M.C. Carrozza, B. Massa, S. Micera, R. Lazzarini, M. Zecca, P. Dario, The development of a novel prosthetic hand-ongoing research and preliminary results, Mechatron. IEEE/ASME Trans. 7 (2) (2002) 108–114.
[7] M.C. Carrozza, C. Suppo, F. Sebastiani, B. Massa, F. Vecchi, R. Lazzarini, M.R. Cutkosky, P. Dario, The SPRING hand: development of a self-adaptive prosthesis for restoring natural grasping, Autonom. Robots 16 (2) (2004) 125–141.
[8] C.T. Yao, M.C. Peckerar, J.H. Wasilik, C. Amazeen, S. Bishop, A novel three-dimensional microstructure fabrication technique for a triaxial tactile sensor array, in: Proceedings of the IEEE Micro-Robotics and Teleoperators Workshop, 1987.
[9] Z. Chu, P.M. Sarro, S. Middelhoek, Silicon three-axial tactile sensor, Sens. Actuators A 54 (1996) 505–510.
[10] L. Wang, D.J. Beebe, A silicon-based shear force sensor: development and characterization, Sens. Actuators 84 (2000) 33–44.
[11] S. Bütefisch, S. Büttgenbach, T. Kleine-Besten, U. Brand, Micromechanical three-axial tactile force sensor for micromaterial characterization, Microsyst. Technol. 7 (2001) 171–174.
[12] B.J. Kane, M.A. Cutkosky, G.T.A. Kovacs, A traction stress sensor array for use in high-resolution robotic tactile imaging, J. Microelectromech. Syst. 9 (4) (2000).
[13] M.S. Bartsch, A. Parridge, B.L. Pruitt, R.J. Full, T.W. Kenny, A three-axis piezoresistive micromachined force sensor for studying cockroach biomechanics, in: Proceedings of the 2000 International Mechanical Engineering Congress and Exposition, 2000, pp. 443–448.
[14] W.L. Jin, C.D. Mote, Development and calibration of a sub-millimeter three-component force sensor, Sens. Actuators A 65 (1998) 89–94.
[15] F. Jiang, Y. Xu, T. Wang, Z. Han, Y. Tai, Flexible shear stress sensor skin for aerodynamics applications, in: Proceedings of 13th IEEE International Conference on Micro Electro Mechanical Systems, MEMS'00.
[16] Y. Xu, F. Jiang, S. Newbern, A. Huang, C. Ho, Y. Tai, Flexible shear-stress sensor skin and its application to unmanned aerial vehicles, Sens. Actuators A 105 (2003) 321–329.
[17] M. Hsieh, Y. Fang, M. Ju, G. Chen, J. Ho, C.H. Yang, P. Wu, G.S. Wu, T. Chen, A contact-type piezoresistive micro-shear stress sensor for above-knee prosthesis application, IEEE J. Microelectromech. Syst. 10 (1) (2001) 121–127.
[18] N.K.S. Lee, R.S. Goonetilleke, Y.S. Cheung, M.Y. So Geommi, A flexible encapsulated MEMS pressure sensor system for biomechanical applications, Microsyst. Technol. 7 (2) (2001) 55–62.
[19] W. Lang, Reflexions on the future of microsystems, Sens. Actuators A 72 (1999) 1–15.
[20] J.W. Judy, Microelectromechanical systems (MEMS): fabrication, design and applications, Smart Mater. Struct. 10 (2001) 1115–1134.
[21] D.J. Beebe, D.D. Denton, A flexible polyimide package for silicon sensors, Sens. Actuators A44 (1994) 57–64.
[22] B. Kloeck, Piezoresistive sensors, in: W. Göpel, J. Hesse, J.N. Zemel (Eds.), Sensors a Comprehensive Survey: Mechanical Sensors, vol. 7, 1994.
[23] G. Westling, R.S. Johansson, Responses in glabrous skin mechanoreceptors during precision grip in humans, Exp. Brain Res. 66 (1987) 128–140.
[24] M. Madou, Fundamentals of Microfabrication, CRC Press, 1997.
[25] R. Bashir, A. Gupta, G.W. Neudeck, M. McElfresh, R. Gomez, On the design of piezoresistive silicon cantilevers with stress concentration regions for scanning probe microscopy applications, J. Micromech. Microeng. 10 (2000) 483–491.
[26] C.S. Smith, Piezoresistance effect in germanium and silicon, Phys. Rev. 94 (1) (1954) 42–49.
[27] Y. Kanda, A graphical representation of the piezoresistance coefficients in silicon, IEEE Trans. Electron Devices 29 (1982) 64–70.
[28] F. Laermer, P. Schilp, Method of anisotropically etching silicon, German Patent DE4241045, 1994.
[29] R. Huber, J. Conrad, L. Schmitt, K. Hecker, J. Scheurer, M. Weber, Microelectron. Eng. 67/68 (2003) 410–416.

Biographies

Lucia Beccai received her Laurea degree in electronic engineering from the University of Pisa in February 1998. She joined the Center of Research in Microengineering (CRIM, formerly MiTech) Laboratory in June 1999 as research assistant. She received her PhD degree in microsystem engineering in March 2003 by discussing a thesis entitled "Design, fabrication and packaging of a silicon based three-axial force sensor for biomedical applications" and now has a post-doctoral position at the CRIM lab of Scuola Superiore Sant'Anna. Dr. Beccai collaborates to several European projects and her research interests are in the fields of microfabrication technologies, microsystems for biomedical applications, and sensory systems' integration in robotics and rehabilitation engineering.

Stefano Roccella received his Laurea degree in aeronautical engineering from the University of Pisa in February 1999. In the same year he joined the Advanced Robotic Technology and System (ARTS) Laboratory of the Scuola Superiore Sant'Anna in Pisa as a research assistant. In March 2003 he started his PhD in robotics at University of Genova. Currently, he is an assistant professor of biomedical robotics at Scuola Sant'Anna, where he is member of the ARTS Lab. His research interests are in the fields of biomedical robotics, rehabilitation engineering, biomechatronics and MEMS design and development.

Alberto Arena received his Laurea degree in electronic engineering from the University of Pisa in 1999. His thesis was focused on the design and a fabrication of a proportional miniaturized valve for biomedical applications, and the final product was patented (Patent No. WO 02/090807). In the same year he joined the CRIM (formerly MiTech Lab) of the Scuola Superiore Sant'Anna (SSSA) in Pisa as research engineer. Since May 2000, he awarded several research grants at SSSA. His main research interests are in the field of biomedical microrobotics, micromechatronics, microelectronics and microsensors. He has been working on many European and international projects for the development of minimally invasive instrumentation for medical applications, and is co-inventor of a system related to locomotion issues for colonoscopy (Patent No. WO 02/068035 A1). Since 2001, he is project manager of the IVP (Intracorporeal Video Probe) Project.

Francesco Valvo received the Laurea degree in electronic engineering from the University of Pisa, in December 1997. He worked at the School of Electronic Engineering and Computer Systems, University of Wales, Bangor (UK) and in 1999 he joined the CRIM Lab of the Scuola Superiore Sant'Anna in Pisa, Italy. His main research interests are in the field of fabrication technology for sensor development.

Pietro Valdastri received his Laurea Degree in electronic engineering (with honors) from the University of Pisa in February 2002. In the same year he joined the CRIM Lab of the Scuola Superiore Sant'Anna in Pisa as a Research Assistant. In January 2003 he started his PhD in bioengineering at CRIM Lab. Main research interests are in the field of implantable biotelemetry, MEMS-based biosensors, and micromanipulation. He is working on several European projects for the development of minimally invasive biomedical devices.

Arianna Menciassi received her Laurea degree in physics (with honors) from the University of Pisa in 1995. In the same year, she joined the MiTech Lab of the Scuola Superiore Sant'Anna in Pisa as a PhD student in bioengineering with a research program on the micromanipulation of mechanical and biological micro objects. In 1999, she received her PhD degree by discussing a thesis titled 'Microfabricated Grippers for Micromanipulation of Biological and Mechanical Objects'. She had a post-doctoral position at SSSA from May 1999 until April 2000. Then, she obtained a temporary position of assistant professor in bioengineering at SSSA. Her main research interests are in the fields of biomedical microrobotics, microfabrication technologies, micromechatronics and microsystem technologies. She is working on several European projects and international projects for the development of minimally invasive instrumentation for medical applications.

Maria Chiara Carrozza received her Laurea degree in physics from the University of Pisa, Italy, in 1990, and the PhD degree in mechanical engineering at Scuola Superiore Sant'Anna, Pisa, Italy, in 1994. Currently, she is an associate professor of biomedical robotics at Scuola Sant'Anna, where she directs the Advanced Robotic Technology and System (ARTS) Laboratory. She is also the scientific manager of the research area of functional replacement at the INAIL/RTR Research Center on Rehabilitation Engineering. Her research interests are in the fields of biomedical microengineering and rehabilitation engineering. Dr. Carrozza is a member of the IEEE Engineering in Medicine and Biology and IEEE Robotics and Automation Societies.

Paolo Dario received his Dr Eng degree in mechanical engineering from the University of Pisa in 1977. Currently, he is a professor of biomedical robotics at the Scuola Superiore Sant'Anna, Pisa. He also established and teaches the course on mechatronics at the School of Engineering, University of Pisa. He has been a visiting professor at the Ecole Polytechnique Federale de Lausanne (EPFL), Lausanne, Switzerland, and at Waseda University, Tokyo, Japan. He is the Director of the Center for Research in Microengineering Laboratory of SSSA, where he supervises a team of about 70 researchers and PhD students. His main research interests are in the fields of medical robotics, mechatronics and microengineering, and specifically in sensors and actuators for the above applications. He is the coordinator of many national and European projects, the editor of two books on the subject of robotics and the author of more than 200 scientific papers. He is a member of the Board of the International Foundation of Robotics Research. He is an associate editor of the *IEEE Transactions on Robotics and Automation*, a member of the Steering Committee of the *Journal of Microelectromechanical Systems* and a guest editor of the Special Issue on Medical Robotics of the *IEEE Transactions on Robotics and Automation*. He serves as President of the IEEE Robotics and Automation Society and as the co-chairman of the Technical Committee on Medical Robotics of the same society.